Ligand-Based Pharmacophore Modeling and Virtual Screening for the Discovery of Novel 17β-Hydroxysteroid Dehydrogenase 2 Inhibitors

Anna Vuorinen,[†] Roger Engeli,[‡] Arne Meyer,[‡] Fabio Bachmann,[‡] Ulrich J. Griesser,[§] Daniela Schuster,*[,†] and Alex Odermatt*[,‡]

[†]Institute of Pharmacy/Pharmaceutical Chemistry and Center for Molecular Biosciences Innsbruck − CMBI, University of Innsbruck, Innrain 80/82, 6020 Innsbruck, Austria

[‡]Swiss Center for Applied Human Toxicology and Division of Molecular and Systems Toxicology, Department of Pharmaceutical Sciences, University of Basel, Klingelbergstrasse 50, 4056 Basel, Switzerland

[§]Institute of Pharmacy/Pharmaceutical Technology, University of Innsbruck, Innrain 52c, 6020 Innsbruck, Austria

S *Supporting Information*
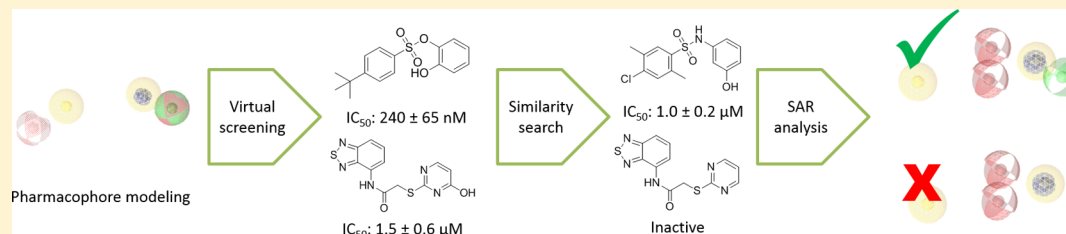
ABSTRACT: 17β-Hydroxysteroid dehydrogenase 2 (17β-HSD2) catalyzes the inactivation of estradiol into estrone. This enzyme is expressed only in a few tissues, and therefore its inhibition is considered as a treatment option for osteoporosis to ameliorate estrogen deficiency. In this study, ligand-based pharmacophore models for 17β-HSD2 inhibitors were constructed and employed for virtual screening. From the virtual screening hits, 29 substances were evaluated in vitro for 17β-HSD2 inhibition. Seven compounds inhibited 17β-HSD2 with low micromolar IC$_{50}$ values. To investigate structure−activity relationships (SAR), 30 more derivatives of the original hits were tested. The three most potent hits, **12**, **22**, and **15**, had IC$_{50}$ values of 240 nM, 1 μM, and 1.5 μM, respectively. All but 1 of the 13 identified inhibitors were selective over 17β-HSD1, the enzyme catalyzing conversion of estrone into estradiol. Three of the new, small, synthetic 17β-HSD2 inhibitors showed acceptable selectivity over other related HSDs, and six of them did not affect other HSDs.

INTRODUCTION

The worldwide prevalence of osteoporosis is high: already in 2006 it was estimated that over 200 million people suffered from this disease.[1] Osteoporosis is defined as a condition, where reduced bone mass and bone density lead to bone fragility and increased fracture risk.[2] Bone density is a result of the balance between osteoblast and osteoclast activities: while osteoblasts are responsible for the formation and mineralization of the bone, osteoclasts play an important role in bone degradation. Bone density is known to decrease in the elderly and is linked to decreased concentrations of sex steroids.[3] Postmenopausal estrogen deficiency promotes osteoporosis in women,[4] and an age-related decrease of testosterone has been associated with osteoporosis in men.[5] It has been shown that both estradiol and testosterone inhibit bone degradation, thereby providing an explanation for the age-related onset of osteoporosis.[6]

To date, there are only few treatment options for osteoporosis: bisphosphonates, which prevent bone loss, selective estrogen receptor modulators (SERMs) such as raloxifene, and hormone replacement therapy that increases circulating estrogen levels.[7,8]

However, all of these therapies have disadvantages. Bisphosphonates need to be orally administered at least 0.5 h before breakfast and any other medication, and the treatment has to be continued for at least three years, which diminishes the patient's compliance.[8] SERMs and hormone-replacement therapies have been associated with cardiovascular complications.[7,8] Besides, hormone replacement therapy increases the risk of breast cancer and is therefore only recommended for patients where a non-hormonal therapy is contraindicated.[9] Because of the limitations related to existing treatments, there is a great demand for novel therapies. One promising approach to overcome the cardiovascular complications and increased breast cancer risk is to increase estradiol concentrations locally in bone cells without altering systemic levels.

The activity of estrogen receptors is dependent on the local availability of active estradiol, which is regulated by the synthesis via aromatase, deconjugation by sulfatase, and conversion from

estrone by 17β-hydroxysteroid dehydrogenase 1 (17β-HSD1).[10] Estradiol is primarily converted to the inactive estrone by 17β-HSD2.[11] Besides its expression in bone cells, 17β-HSD2 is localized only in a few tissues, including placenta,[12] endometrium,[13] prostate,[14] and small intestine epithelium.[15] Thus, inhibition of 17β-HSD2 may be a suitable way to increase estradiol levels without raising breast cancer and cardiovascular risks. Indeed, there is support from in vivo studies that 17β-HSD2 could be a target for the treatment of osteoporosis. In ovariectomized monkeys, oral administration of a 17β-HSD2 inhibitor increased bone strength by elevating bone formation and decreasing bone resorption.[16]

In addition to the oxidative inactivation of estradiol to estrone, 17β-HSD2 was reported to convert testosterone into 4-androstene-3,17-dione (androstenedione), dihydrotestosterone into 5α-androstanedione, and 5α-androstenediol into dehydroepiandrosterone (Figure 1).[17,18] It can also adopt 20-hydroxysteroids
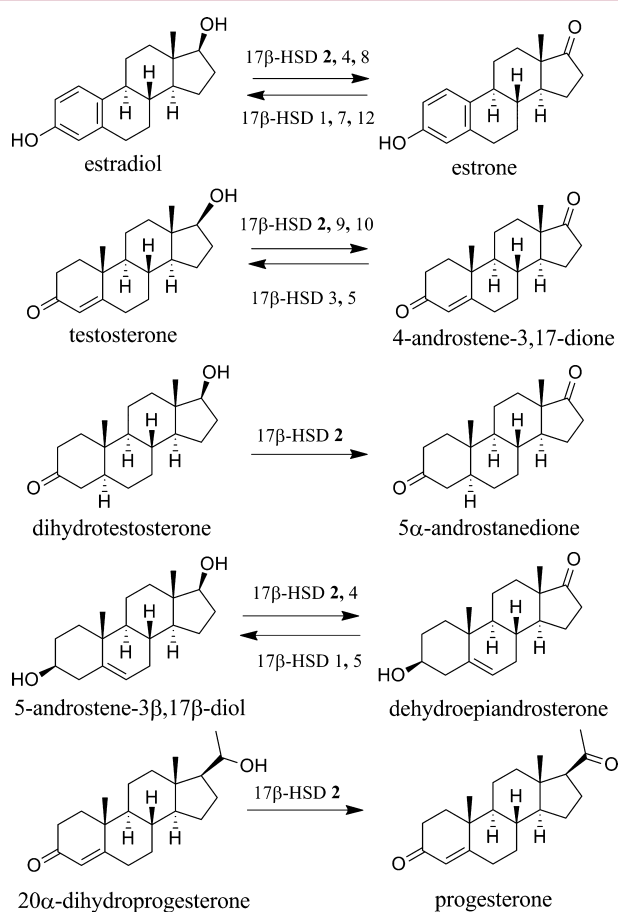
**Figure 1.** Sex steroid metabolism catalyzed by 17β-HSD2 and other 17β-HSDs.

as substrates and convert 20α-dihydroprogesterone into progesterone (Figure 1).[17] 17β-HSD2 is an NAD+-dependent microsomal membrane enzyme.[18,19] It belongs to the short-chain dehydrogenases (SDRs), an enzyme family of oxidoreductases comprising at least 72 different genes in humans.[20,21] Members of this family share a similar protein folding, the so-called "Rossman-fold", where six or seven β-sheets are surrounded by three to four α-helices.[21] Even though the sequence identities of SDRs are low, often less than 20%, they share a conserved glycine-rich area in the cofactor binding site and a Tyr-X-X-X-Lys motif in the active site. Despite the low sequence identities, the

SDRs are well superimposable in 3D and their active site structures are similar.[21] Thus, when developing inhibitors for one of the SDRs, the selectivity of the compounds over the other related enzymes should be evaluated.

In recent years, several potent and selective 17β-HSD2 inhibitors (e.g., **1–4**, Figure 2) have been reported.[22−25] Some of
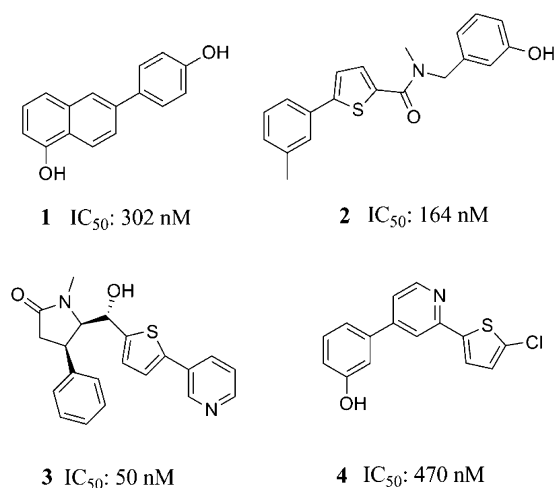

Figure 2. Previously reported 17β-HSD2 inhibitors.[22−25]

these compounds (such as **4**) have been discovered during the search for selective 17β-HSD1 inhibitors by synthetizing estrone-mimicking compounds.[25] Most of these compounds were steroid mimetics or developed rationally by structure–activity-relationship (SAR) studies.[22,23,26,27] The starting structure for the SAR studies had been a previously developed inhibitor (**3**) or a promising scaffold such as flavonoids that represent the basis for compound **1**.[23] Because most of the known inhibitors are based on estrone-mimicking compounds or previously developed inhibitors, they often are similar in size, are derived from the same scaffold, or include analogue bioisosteric groups. For this reason, there is a need for novel scaffolds and inhibitors that could serve as starting points for further drug development. We approached the search for novel, chemically diverse 17β-HSD2 inhibitors by ligand-based pharmacophore modeling and virtual screening.

Pharmacophore models represent the 3D-arrangement of the chemical features and steric limitations that are necessary for a small molecule to interact with a specific target protein.[28] These features correspond to chemical functionalities such as hydrogen bond acceptors (HBAs), hydrogen bond donors (HBDs), hydrophobic areas (Hs), aromatic rings (ARs), positively/negatively ionizable groups (PIs/NIs), and exclusion volumes (XVOLs). Pharmacophore models are widely used as virtual screening filters.[29] A result of a virtual screening is a so-called hit list containing compounds with functional groups that map the pharmacophore model. These compounds are predicted to be active against a specific target. In this study, we report the development of a pharmacophore model for 17β-HSD2 inhibitors and its use in a virtual screening campaign. From the virtual hit lists, 29 compounds were biologically evaluated, of which 7 showed activities in the low micromolar range. As follow-up, we focused on one scaffold and tested similar compounds to get insights into their SAR.

■ RESULTS

Due to the lack of an experimentally determined 3D-structure of 17β-HSD2, a ligand-based pharmacophore modeling approach
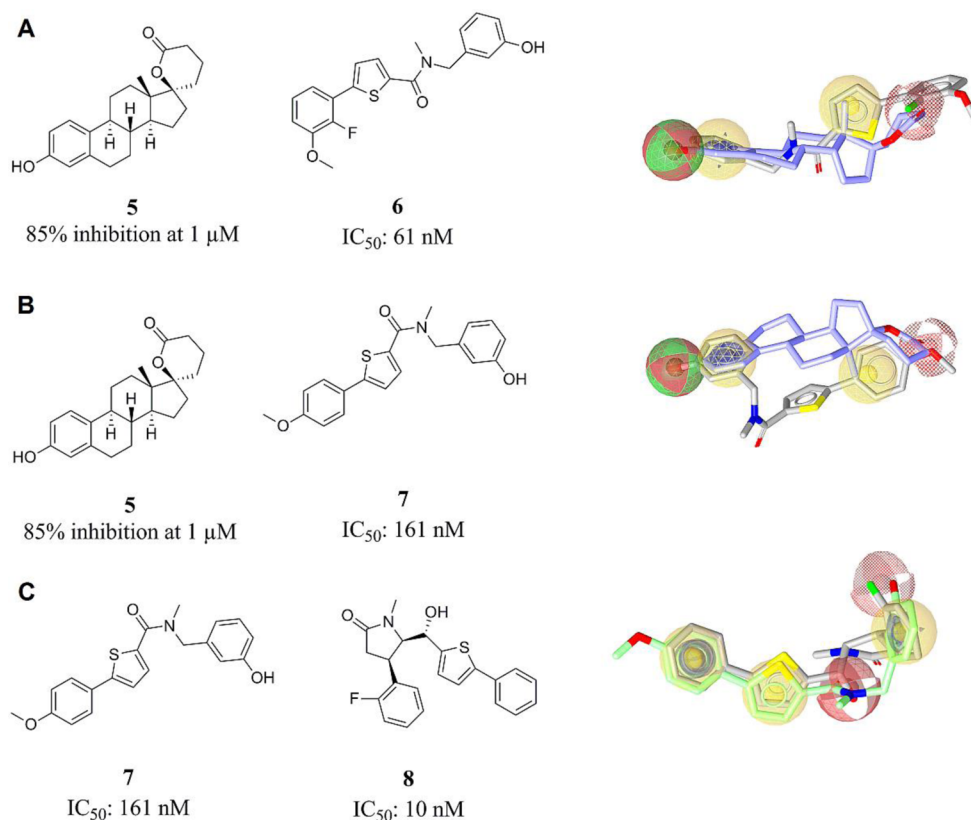
Figure 3. Pharmacophore models 1 (A), 2 (B), and 3 (C) for 17β-HSD2 inhibition with their training compounds. On the left-hand side, the training compounds are represented as 2D structures with their activities. On the right-hand side, the training compounds are aligned with the chemical features of the respective models. The pharmacophore features are color-coded: HBA, red; HBD, green; H, yellow; AR, blue. Optional features are shown in scattered style. For clarity, the XVOLs are not depicted.
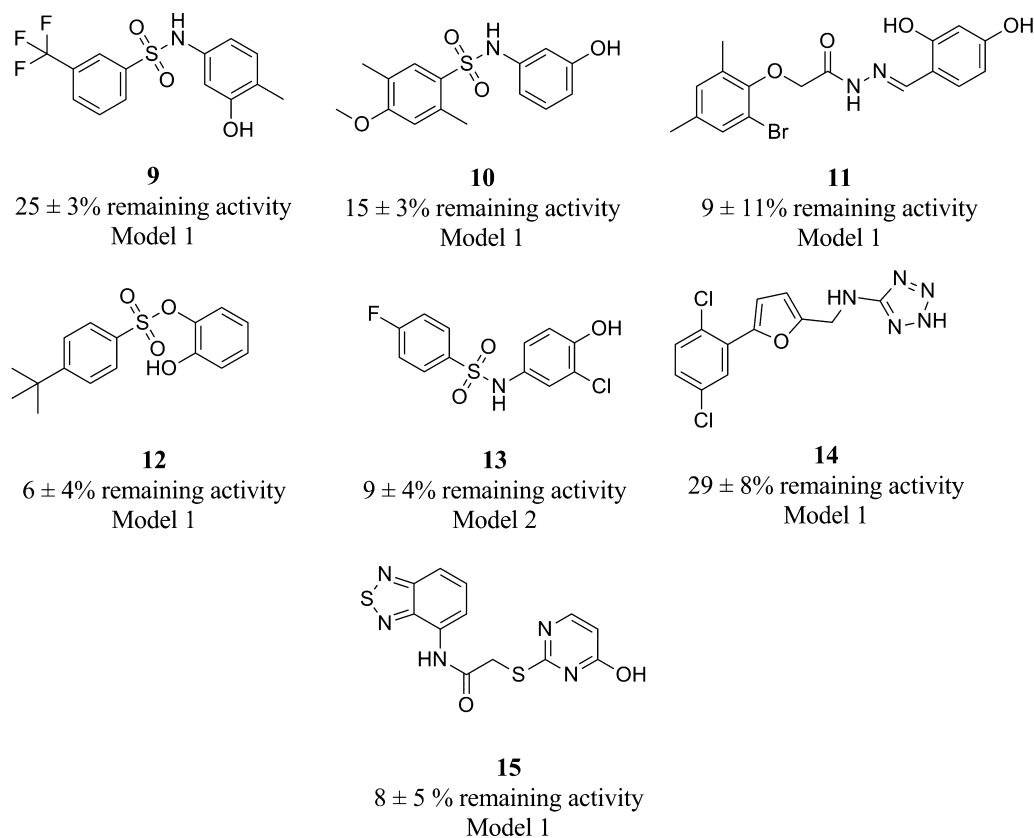
was chosen. In this method, a model is based on the common chemical features of already known active compounds. After construction, the newly generated pharmacophore model is refined to recognize only the active compounds from a so-called test set, containing previously known active and inactive compounds. The theoretical model quality can be described quantitatively by its specificity and selectivity, which are defined by the retrieval of active and inactive compounds, respectively. Often an increase in specificity decreases the sensitivity: a model that finds all active compounds might also find multiple inactive compounds. Therefore, constructing a good pharmacophore model requires balancing between specificity and sensitivity. We aimed to overcome this fact by the parallel use of several restrictive models, complementing each other in their hit lists.[30] Using several restrictive models, we aimed to achieve the best overall enrichment of active compounds from the test set without finding a large number of inactive entries.

All generated models were based on the common chemical features of two training compounds, respectively, that were collected from the literature: model 1 on **5**[31] and **6**,[22] model 2 on **5** and **7**,[22] and model 3 on **7** and **8**,[24] respectively (Figure 3). The selection of these two molecules as training sets for each model was based on their structural diversity and potency. The automatically created common feature pharmacophore models were refined by removing features, adjusting the XVOL size, and setting features optional to correctly recognize the active compounds from the test set containing 15 active and 30 inactive compounds (Supporting Information, Table S1). The general workflow for model refinement has been described previously.[32]

Model 1 consisted of six features: two H, one HBD, one AR, and two HBAs, of which one was set optional, and 54 XVOLs (Figure 3A). This model was able to recognize eight active but no inactive compounds from the test set. Model 2 consisted of the same features as model 1, but with different spatial arrangement (Figure 3B). This model also recognized eight active compounds, of which five were common with model 1, but no inactive compounds from the test set. Model 3 consisted of seven features: three Hs, two ARs, two HBAs, of which one was set optional, and 56 XVOLs (Figure 3C). This model was more restrictive than the other two: it found six active but no inactive compounds from the test set screening. Together, these three models were able to correctly retrieve 13 active compounds from the test set, representing 87% of all the actives (overall sensitivity: 0.87. Sensitivity of models 1 and 2: 0.53, respectively, and model 3: 0.4). Remarkably, not a single inactive compound was found.

Because the combined retrieval of the active compounds from the test set was encouraging, the three models were employed for virtual screening of the SPECS database including 202 906 small molecules (www.specs.net). Models 1, 2, and 3 returned 573, 825, and 318 hits, respectively. In total, 1716 hits were obtained, of which 185 molecules were found by two models. Without duplicates, our models retrieved 1531 hits, representing 0.75% of all the compounds in the database. To separate the druglike compounds from the others, all the hit lists were filtered using a modified Lipinski filter,[33] resulting in total of 1381 unique, druglike hits.

From each hit list, the ten top-ranked hits were considered for further analysis. However, these top hits often contained chemically very similar hits. To get more diverse hits for

9
25 ± 3% remaining activity
Model 1

10
15 ± 3% remaining activity
Model 1

11
9 ± 11% remaining activity
Model 1

12
6 ± 4% remaining activity
Model 1

13
9 ± 4% remaining activity
Model 2

14
29 ± 8% remaining activity
Model 1

15
8 ± 5 % remaining activity
Model 1

Figure 4. Seven newly discovered 17β-HSD2 inhibitors with their activities and mapping pharmacophore models. Activities are given as remaining enzyme activity (% of control) at an inhibitor concentration of 20 μM in a cell-free assay.

Table 1. Inhibitory Activities (IC$_{50}$) of the Seven Newly Discovered Inhibitors against 17β-HSD2 and Related HSDs

compd	17β-HSD2 lysate	17β-HSD2 intact	17β-HSD1 lysate	11β-HSD1 lysate	11β-HSD2 lysate	17β-HSD3 intact
9	7.1 ± 0.4 μM	n.d.[a]	n.i.[b]	n.i.	n.i.	n.i.
10	6.9 ± 3.5 μM	n.d.	n.i.	n.i.	n.i.	n.i.
11	4.1 ± 1.4 μM	23 ± 3 μM	52 ± 15%[c]	69 ± 2%	61 ± 3%	1.6 ± 0.8 μM
12	240 ± 65 nM	520 ± 210 nM	n.i.	2.1 ± 0.7 μM	n.i.	8.5 ± 3.5 μM
13	3.0 ± 1.5 μM	10 ± 1 μM	n.i.	n.i.	n.i.	3.9 ± 1.2 μM
14	33 ± 5 μM	n.d.	n.i.	n.i.	n.i.	n.i.
15	1.5 ± 0.6 μM	1.1 ± 0.1 μM	n.i.	n.i.	n.i.	n.i.

[a]n.d. = not determined. [b]n.i = no inhibition (rest activity >70% at the concentration of 20 μM). [c]% rest activity at 20 μM.

biological testing, for each hit list 10 clusters were calculated. Out of each cluster, the 3 best-ranked compounds were kept. The preferred compounds list finally contained 73 unique hits. Among them, 3 were consensus hits of two models and therefore selected for biological evaluation. The other compounds were selected based on their overall fit score and a preferentially high fit score within their cluster. Finally, the OSIRIS property explorer (www.organic-chemistry.org/prog/peo[34]) was used to predict druglikeness, mutagenicity, irritant, and tumorigenic effects of the compounds. Only compounds passing this filter were considered for further research. Giving preference for the best ranked compounds from the filtered hit lists, 2 consensus hits mapping the models 1 and 2, 10 compounds mapping model 1, 8 compounds fitting to model 2, and 9 compounds fitting model 3 were selected. In summary, the selection was based on compound druglikeness, pharmacophore fit score, chemical diversity, and availability. The chemical structures of all selected compounds with their pharmacophore fit scores and ranks in the hit lists are available in the Supporting Information, Table S2.

Next, the 17β-HSD2 inhibitory activities of the chosen hits were evaluated in a cell-free assay. The activities were first determined at an inhibitor concentration of 20 μM using lysates of transfected HEK-293 cells. In all experiments, vehicle was included as negative control and *N*-(3-methoxyphenyl)-*N*-methyl-5-*m*-tolylthiophene-2-carboxamide (compound **19** from ref 26) as positive control. Of the newly predicted 29 compounds, 7 showed more than 70% enzyme inhibition (Figure 4), which corresponds to a 24% true positive hit rate. The other compounds were inactive or weakly active (data not shown).

The seven active compounds (**9**−**15**) were further biologically evaluated. First, the IC$_{50}$ values were determined in the cell-free assay (Table 1). Irreversible inhibition was excluded by comparing enzyme activity upon preincubation of the enzyme preparation with the inhibitor of interest for 10 and 30 min with that after simultaneous incubation.[35] Promiscuous enzyme inhibition due to aggregate formation of the chemicals was excluded by comparing activities in the absence and presence of 0.1% Triton X-100.[36] Structurally, most of the active compounds
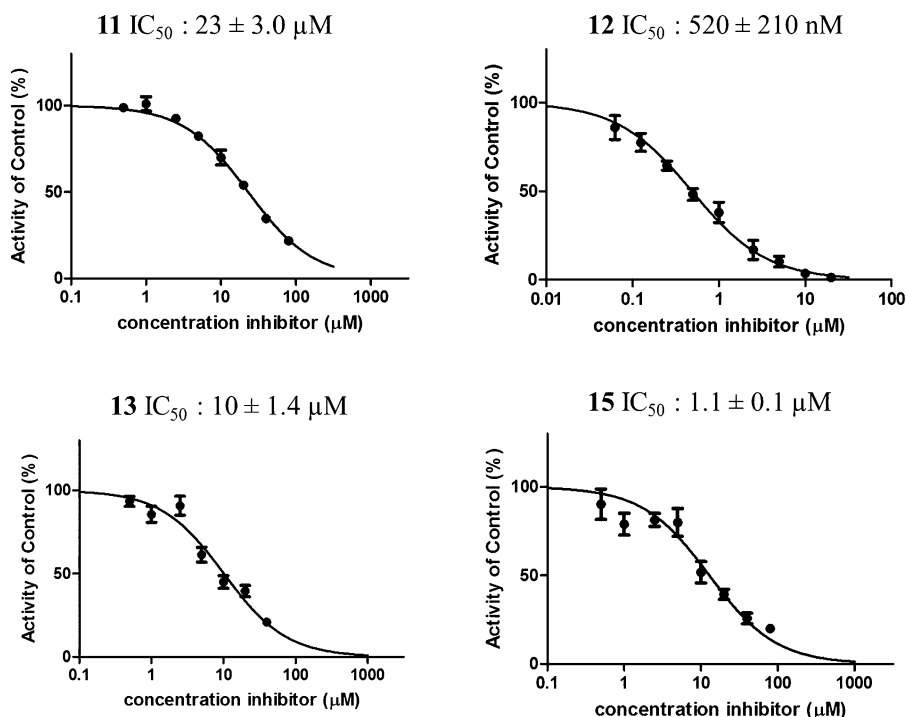
11 $IC_{50} : 23 \pm 3.0 \ \mu M$

12 $IC_{50} : 520 \pm 210 \ nM$

13 $IC_{50} : 10 \pm 1.4 \ \mu M$

15 $IC_{50} : 1.1 \pm 0.1 \ \mu M$

Figure 5. IC_{50} determinations for compounds **11−13** and **15** in intact cells ($n = 3−5$).

shared a sulfonamide or sulfonic acid ester linker between two benzene rings. The remaining three active compounds represented other chemical classes. To the best of our knowledge, similar compounds or the same chemical scaffolds have not been reported previously as 17β-HSD2 inhibitors.

The compounds with IC_{50} values below 5 μM in lysed cells were tested in intact HEK-293 cells transfected with 17β-HSD2. The four compounds (**11**, **12**, **13**, and **15**) concentration-dependently inhibited 17β-HSD2 (Figure 5). The two most potent inhibitors, **12** and **15**, had IC_{50} values of 520 $\pm$ 210 nM and 1.1 $\pm$ 0.1 μM, respectively. Compound **15** had comparable IC_{50} values for 17β-HSD2 in intact and in lysed cells. For compound **14**, the initial enzyme inhibition tests at the concentration 20 μM yielded a remaining activity of 29 $\pm$ 8%. However, the IC_{50} for this compound was higher than the initial tests led to expect. The reason for this high IC_{50} value is unclear but may be due to limited solubility and/or stability of the compound.
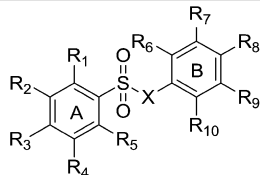
Because of the structural similarity to related HSDs and their common intracellular localization at the ER membrane, the seven most active compounds were evaluated for inhibitory activities against other HSDs: (i) 17β-HSD1 catalyzing the conversion of estrone into estradiol (Figure 1), (ii) 11β-HSD1 and -2 that are responsible for the interconversion of glucocorticoids,[37] and (iii) 17β-HSD3 that converts androstenedione to testosterone (Figure 1).[38] The enzyme activity of 17β-HSD3 was assessed in intact cells because the activity declines rapidly upon cell lysis; therefore, the relative inhibition of the compounds might be affected by their ability to enter the intact cell. IC_{50} values were determined for compounds with an inhibitory activity of at least 70% at a compound concentration of 20 μM. Otherwise, the compound was considered as inactive. The results of the selectivity studies are presented in Table 1. Compounds **9**, **10**, **14**, and **15** turned out to be selective over the other tested HSDs. Importantly, all compounds were selective over 17β-HSD1. However, compound **12** inhibited 11β-HSD1 and 17β-HSD3

with IC_{50} values of 2.1 $\pm$ 0.7 μM and 8.5 $\pm$ 3.5 μM, respectively. Compounds **11** and **13** showed equal or more potent inhibition of 17β-HSD3 with IC_{50} values below 5 μM.
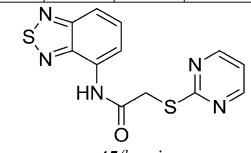
Inspired by the new inhibitors, we searched for compounds similar to the new 17β-HSD2 inhibitors in the SPECS database, especially focusing on the phenylbenzenesulfonamide and phenylbenzenesulfonate scaffolds. The aim of the similarity search was to generate a SAR for this scaffold. The similarity search was approached from two ways: (i) plain 2D similarity search for all the new inhibitors without fitting the compounds into the pharmacophore models prior to purchasing them and (ii) search for similar compounds in the SPECS database via virtual screening using model 1, which found the originally active phenylbenzenesulfonamides and phenylbenzenesulfonates.

Altogether, 30 compounds were selected for the biological analysis (Table 2). Sixteen of them were selected just based on their structural similarity to active compounds, and 14 were picked from the virtual screening hits. From the 16 compounds that were selected because of plain 2D similarity, only one compound, **16**, inhibited 17β-HSD2 with an IC_{50} value of 3.3 $\pm$ 1.2 μM. The other tested compounds (**17−19**, **25−28**, **21−24**, **32−35**, and **45−48**), independent of their high structural similarity to the original hits (**9−15**), showed only weak or no activity (Table 2). However, among the compounds selected by model 1, several substances were active: five inhibited 17β-HSD2 with IC_{50} values between 1 and 15 μM, three had weak activity (50−70% inhibition at 20 μM), two were not tested because they were insoluble in commonly used solvents, and the remaining four compounds were inactive (Table 2).
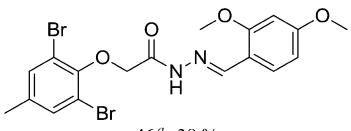
These active inhibitor-derivatives were also tested against other related HSDs (Table 3). Compound **22** was the only compound with weak activity on 17β-HSD1; however, it was still 18-fold more active toward 17β-HSD2. Compounds **20** and **23** were almost equipotent toward 17β-HSD2 and 11β-HSD1. Compounds **16** and **22** were weak 17β-HSD3 inhibitors, while the other derivatives did not have effect on this enzyme.

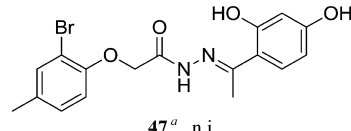**Table 2. Phenylbenzenesulfonamides and -sulfonates with Their 17β-HSD2 Inhibitory Activities**

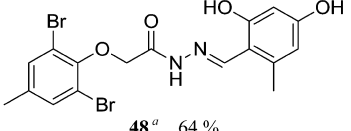| Comp.	X	R1	R2	R3	R4	R5	R6	R7	R8	R9	R10	IC$_{50}$
9	NH	H	CF$_3$	H	H	H	H	H	CH$_3$	OH	H	7.1 µM
10	NH	H	CH$_3$	OCH$_3$	H	CH$_3$	H	OH	H	H	H	6.9 µM
12	O	H	H	Tert-But	H	H	H	H	H	H	OH	240 nM
13	NH	H	H	F	H	H	H	H	OH	Cl	H	3.0 µM
16[a]	NH	CH$_3$	H	CH$_3$	CH$_3$	H	H	OH	H	H	H	3.3 µM
17[a]	O	H	H	Tert-But	H	H	H	H	H	H	OCH$_3$	51 %[b]
18[a]	NH	H	H	F	H	H	H	H	H	Cl	H	n.i.[c]
19[a]	NH	H	H	OCH$_3$	H	H	H	H	CH$_3$	OH	H	47 %
20	NH	H	H	OCH$_3$	H	H	CH$_2$CH$_2$CH$_2$CH$_2$	OH	H	H		9.6 µM
21	NH	H	H	Br	H	H	H	H	H	OH	H	4.9 µM
22	NH	H	CH$_3$	Cl	H	CH$_3$	H	H	H	OH	H	1.0 µM
23	NH	CH$_2$CH$_2$CH$_2$CH$_2$	OCH$_3$	H	H	H	H	H	H	OH	H	15 µM
24	NH	H	Br	H	H	H	H	H	CH$_3$	OH	H	6.3 µM
25[a]	NH	CH$_3$	H	H	CH$_3$	H	H	H	OCH$_3$	H	H	n.i.
26[a]	NH	CH$_2$CH$_3$	H	H	CH$_2$CH$_3$	H	H	OCH$_3$	H	H	OCH$_3$	n.i.
27[a]	NH	CH$_3$	H	OCH$_3$	CH$_3$	H	H	H	COOH	H	H	n.i.
28[a]	NH	CH$_3$	H	OCH$_3$	CH$_3$	H	H	H	Cl	H	H	n.i.
29	NH	CH$_3$	H	CH$_3$	H	CH$_3$	H	H	OH	H	H	33 %
30	NH	CH$_3$	H	H	CH$_3$	H	H	H	OH	H	H	39 %
31	NH	H	H	Cl	H	H	H	H	CH$_3$	OH	H	45 %
32[a]	NH	H	H	Cl	H	H	H	H	OH	H	H	55 %
33[a]	NH	H	H	F	H	H	H	Cl	H	H	CH$_3$	n.i.
34[a]	NH	H	H	Cl	H	H	H	H	OCH$_3$	H	H	n.i.
35[a]	NH	H	CH$_3$	F	H	H	H	Cl	H	H	OH	44 %
36	O	H	H	NHCOCH$_3$	H	H	H	NCH$_2$CH$_2$CH$_2$	H	H		n.i.
37	O	H	CH$_3$	CH$_3$	H	H	H	H	H	H	NHCOCH$_3$	n.i.
38	O	H	H	NHCOCH$_3$	H	H	H	H	H	H	OCH$_3$	n.i.
39	O	H	H	NHCOCH$_3$	H	H	H	H	COCH$_2$CH$_3$	H	H	67 %
40	NH	H	H	F	H	H	H	H	F	Cl	H	45 %
41	NH	H	H	Br	H	H	H	H	H	F	H	n.i.
42	NH	H	H	Cl	H	H	H	H	H	H	CH2OH	n.i.
43	NH	H	H	F	H	H	H	H	H	H	CHOHCH$_3$	n.i.
44	NH	CH$_3$	CH$_3$	H	CH$_3$	CH$_3$	H	H	H	H	NHCOCH$_3$	n.i.

45[a] n.i.

46[a] 38 %

47[a] n.i.

48[a] 64 %

[a]Compound found by similarity search without fitting it to model 1. [b]17β-HSD2 rest activity given as % of control at an inhibitor concentration of 20 µM. [c]n.i. = no inhibition (rest activity >70% at the concentration of 20 µM).

With all the activity data from the phenylbenzenesulfonamides and -sulfonates, SAR rules were deduced. The SAR analysis confirmed that the HBD functionality is essential for the 17β-HSD2 inhibitory activity. In all the active compounds, except for the weak inhibitors **39** and **46**, this functionality is a phenolic OH group that is an attractive metabolism site. Therefore, five other compounds (**40**–**44**) were purchased and biologically evaluated. In two of these compounds (**40** and **41**) the hydroxyl group was

Table 3. Inhibitory Activities of Active Phenylbenzenesulfonamide and -sulfonate Derivatives Toward 17β-HSD2 and Related HSDs

compd	17β-HSD2 lysate	17β-HSD1 lysate	11β-HSD1 lysate	11β-HSD2 lysate	17β-HSD3 intact
16	3.3 ± 1.2 μM	n.i.[a]	n.i.	n.i.	43 ± 4%[b]
20	9.6 ± 0.4 μM	n.i.	8.1 ± 1.9 μM	n.i.	n.i
21	4.9 ± 0.9 μM	n.i.	n.i.	n.i.	n.i
22	1.0 ± 0.2 μM	18 ± 2 μM	n.i.	n.i.	53 ± 4%
23	15 ± 2 μM	53 ± 5%	13 ± 3 μM	n.i.	n.i
24	6.3 ± 1.1 μM	58 ± 3%	n.i.	n.i.	n.i

[a] n.i. = no inhibition (rest activity >70% at the concentration of 20 μM). [b] % rest activity at 20 μM.

replaced by fluorine, whereas the other three had a hydroxymethyl, 1-hydroxyethyl, or acetamide moiety. None of these compounds were active, which confirms the importance of the HBD feature being directly attached to ring B. Compounds **40** and **41**, where the HBD functionality was replaced by an HBA, were inactive and weakly active, in comparsion to the active compounds **13** and **21**, in which the substitution pattern was otherwise identical with **40** and **41**. In case of the compounds **42−44**, the HBD functionality was present but not directly attached to the ring B. Unfortunately, no amine substitution of the OH group was available, so this option could not be tested. Either the inactivity of these compounds was caused by spacious substituents in ring B or was caused by different substitution patterns in ring A. To derive further information on this scaffold, a further medicinal chemistry study with a full synthesis series would be required.

In addition to just comparing the 2D-structures of the compounds, a ligand-based pharmacophore model from compounds **9**, **10**, **12**, and **13** was developed. The automatically generated model consisted of two Hs, one AR, two HBAs, and 42 XVOLs (Figure 6A). However, a comparison of the 2D-structures of the active compounds revealed that an HBD functionality on B-ring is essential for the activity. Fitting of the training compounds into the model also showed an overlay of hydroxyl groups in the respective area. Therefore, an HBD-feature was manually added to the model (Figure 6B). After fitting all the tested phenylbenzenesulfonamides and -sulfonates to this model, one new XVOL was placed near the HBD functionality to make the model more restrictive toward compounds with too spacious substituents (Figure 6C).

All the phenylbenzenesulfonamides and -sulfonates were fitted to the SAR models. As expected, the model without the HBD feature (Figure 6A) found 11 of the active but also all of the inactive and weakly active compounds. In comparison, the model where the HBD feature was manually added (Figure 6B) found 9 of the active hits, 2 weakly active and 2 inactive compounds. Once the new space restriction was added, (Figure 6C) 9 active and only 2 weakly active compounds fitted to the model. These results emphasized that phenylbenzenesulfonamides and -sulfonates need to have an HBD functionality attached to the B-benzene ring to inhibit 17β-HSD2. When the HBD is part qof a more spacious substituent (e.g., in an amide), activity is decreased.

Finally, the quality of the original 17β-HSD2 pharmacophore models (models 1−3) was evaluated. Therefore, all 28 tested derivatives were fitted into the models to (i) evaluate the model qualities and (ii) to deduce and confirm activity rules from the obtained alignments with the models. In summary, model 1 found 15 phenylbenzenesulfonamides and -sulfonates, of which six (**19**, **20−24**) were active or weakly active. When screening without any space restrictions (XVOLs), compound **16** and
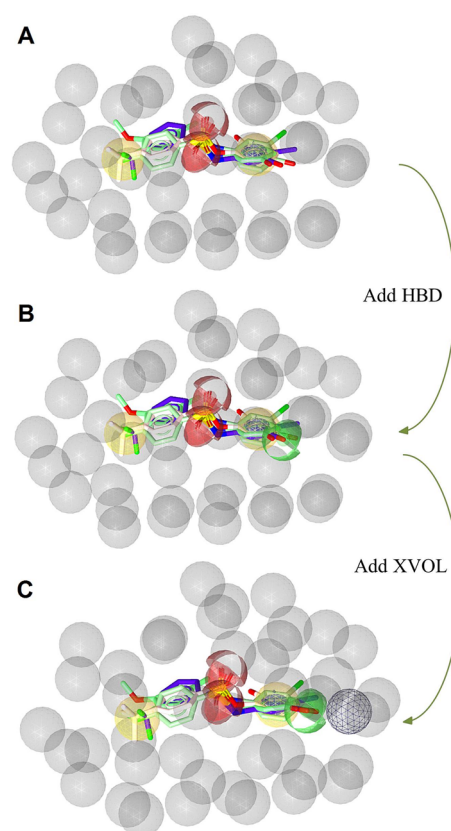
Figure 6. SAR models for 17β-HSD2 inhibiting phenylbenzenesulfonamides and -sulfonates. Automatically generated, ligand-based pharmacophore model (A), manually optimized model (B), and optimized model with space restrictions, added XVOL highlighted (C). Pharmacophore features are color coded: HBA, red; HBD, green; H, yellow; AR, blue; XVOL, gray.

three inactive compounds fitted into model 1 as well. Because model 1 performed well in finding active compounds, but also mapped a number of inactive ones, a possible refinement step could be an optimization of the space restrictions so that the specificity of the model improves. Model 2, in contrast, found the active compounds **16** and **22−24**. Additionally, one weakly active derivative and two inactive compounds mapped to this model. None of the derivatives fitted to model 3.

Because model 1 performed well in finding active compounds, but also mapped a number of inactive ones, it was chosen to be refined for higher specificity. For this purpose, the original test set comprising 15 active and 30 inactive compounds and the 13 active and 43 inactive compounds from the newly generated data were gathered to form a refinement database. All in all, model 1 correctly recognized 19 active compounds from the refinement database but found also 15 inactive compounds. The model's

specificity was then increased by adding new XVOLs as spatial restrictions to the model. In total, 7 new XVOLs were added in the regions, where the inactive molecules were located, but the actives did not protrude into this space. In the end, the refined model 1 found 19 active and 4 inactive compounds. To see how the model performed over a larger database, the SPECS database was screened again. The refined model returned 193 hits, in comparison to the 573 hits of the original model. Thus, the spatial refinement of model 1 drastically decreased the number of hits. This decreased number of hits may indicate an improvement in the models specificity and sensitivity and in its ability to enrich active compound from a database.

■ DISCUSSION

This study aimed to identify new 17β-HSD2 inhibitors by ligand-based pharmacophore modeling. In the course of this study, three specific 17β-HSD2 pharmacophore models were developed and used in combination for prioritizing test compounds from the commercial SPECS database. Initially, 29 compounds from a total of 1381 hit molecules were selected for biological evaluation. Of these compounds, seven inhibited 17β-HSD2 activity more than 70% at a concentration of 20 μM when assayed in lysed cells. In total, this yielded a 24% success rate for these pharmacophore models. A further search for similar compounds resulted in 30 small molecules, which were also tested against 17β-HSD2. Six of these compounds inhibited 17β-HSD2 by more than 70% at a concentration of 20 μM, nine were weak inhibitors (40−69% inhibition at 20 μM concentration), and the remaining compounds were inactive or insoluble. The remaining 28 compounds were then used to evaluate the pharmacophore model quality and derive an SAR model for phenylbenzenesulfonamide and -sulfonate type inhibitors of 17β-HSD2.

Because the original hit compounds were picked from the database by three separate models, the predictive power for each model was analyzed separately. Twelve of the biologically evaluated compounds were picked by model 1, and six of them turned out to be 17β-HSD2 inhibitors. This results in a success rate of 50%, which is very good for an unrefined model. In contrast, the predictive power of models 2 and 3 were moderate: one of the ten compounds selected by model 2 was active. None of the nine compounds picked by model 3 inhibited 17β-HSD2, yielding success rates of 10% and 0%, respectively.

The experimental validation of the models confirmed that the performance of model 1 was excellent, whereas that of models 2 and 3 should be improved if they will be used for further virtual screening studies. A further refinement of model 1 should render it more restrictive and thereby reduce the overall number of hits. However, in light of the obtained screening results, model 1 already showed good predictive power even within one scaffold. In addition, the results that most of the active compounds fit to model 1 and the structurally similar inactive derivatives do not supports the usage of pharmacophore modeling as a method for prioritizing compounds for in vitro assays.

During this study, 13 new 17β-HSD2 inhibitors were discovered. Two of these compounds were previously reported in the literature: **9** is a reagent in the preparation of translation initiation inhibitors,[39] and **20** is a substructure for protein kinase and angiogenesis inhibitors for cancer treatment.[40] For the other new 17β-HSD2 inhibitors, no references were found. The two studies mentioning compounds **9** and **20** described them as intermediate or substructures but not as actual endproducts, and no biological activity was reported for them. Eleven out of the 13 novel 17β-HSD2 inhibitors had IC$_{50}$ values lower than 10 μM,

and the most potent hit **12** had a nanomolar IC$_{50}$ value. Because the first virtual screening revealed phenylbenzenesulfonates and phenylbenzenesulfonamides as promising hits, this scaffold was further explored and six additional 17β-HSD2 inhibitors were discovered. Therefore, a new validated scaffold for 17β-HSD2 inhibitors can be reported.

The similarities in the 3D-folding, functions, and intracellular location of related HSDs make it difficult to predict the selectivity of compounds active against an individual member of this enzyme family. Although the pharmacophore models were based on inhibitors that were selective against 17β-HSD1, the selectivity of the hits needed to be experimentally confirmed. Therefore, selectivity studies for the newly identified 17β-HSD2 inhibitors were performed. Twelve of the 13 discovered inhibitors were selective over 17β-HSD1, which is important regarding treatment of osteoporosis. The only hit that showed activity 17β-HSD1 activity, compound **22**, inhibited 17β-HSD1 with an IC$_{50}$ value of 18 μM, thus being 18 times more active against 17β-HSD2. Compound **22** is similar to compound **10**, however, where **22** has chlorine, and **10** has a methoxy substituent. This suggests that 17β-HSD2 may tolerate more spacious groups in this region. Importantly, all compounds were selective over 11β-HSD2, an antitarget associated with cardiovascular complications such as hypertension and hypokalemia.[37,41] Unfortunately, the most active hit **12** inhibited 11β-HSD1 and 17β-HSD3, with 9-fold and 35-fold selectivity against 17β-HSD2, respectively. Because other compounds from the same scaffold (compounds **9**, **10**, **16**, **21**, and **24**) that were selective over the other tested HSDs were discovered, it may be possible to optimize the selectivity of **12**. In addition, compounds **20** and **23** were equipotent 17β-HSD2 and 11β-HSD1 inhibitors. However, 11β-HSD1 is considered as an antidiabetic target,[42] and its inhibition may actually have beneficial effects in patients suffering from osteoporosis.

Unfortunately, compound **11** turned out to be more active against 17β-HSD3 than 17β-HSD2 and **13** was equipotent toward these two enzymes. Compounds **16** and **26** showed weak activity on 17β-HSD3. 17β-HSD3 is responsible for gonadal testosterone production, and its proper function is essential for fetal development and during puberty.[38] Because osteoporosis usually arises among the elderly, inhibition of 17β-HSD3 may not lead to severe adverse effects. In addition, because this enzyme is expressed almost exclusively in testis[43] and in prostate cancer tissues,[44] its inhibition is not expected to cause adverse effects in postmenopausal patients.

The crystal structure of 17β-HSD2 is not known, but for 17β-HSD1, there are multiple crystal structures available in the Protein Data Bank (PDB, www.pdb.org,[45]). Therefore, the generated pharmacophore models and active compounds of this study were analyzed against the 17β-HSD1 structure (PDB code 3HB5[46]). Model 1 as well as the established SAR model aligned remarkably well with the cocrystallized estradiol derivative. The alignment of the phenylbenzenesulfonates and phenylbenzene-sulfonamides with model 1 in the 17β-HSD1 binding pocket does not explain the compound's selectivities. Interestingly, in the binding site of 17β-HSD1, there are two hydrophobic residues, Leu149 and Val225, that may cause unfavorable interactions with the sulfonamide core of most 17β-HSD2-active compounds. However, this does not explain why compound **22** inhibits 17β-HSD1 but compound **10** does not. Precise conclusions regarding the selectivity cannot be drawn without a crystal structure or a high quality homology model of 17β-HSD2.

In the end, 13 novel 17β-HSD2 inhibitors were discovered during this study. Compound **15**, which was the most potent and

selective hit, was 5-fold less potent than the most active hit, making it a promising lead candidate. All of the identified 17β-HSD2 inhibitors are small molecules that can be easily optimized by ring substitution or bioisosteric replacements for better biological efficacy and/or selectivity.

Even though half of the in vitro evaluated derivatives were not active or were weak inhibitors, some precious information on our models and on the 17β-HSD2 binding site could be derived. Most of the inactive compounds did not fit to the pharmacophore models and especially model 1 was able to enrich the active compounds even within one scaffold. Structural analysis of the identified inhibitors and the derivatives suggested that the hydrogen bond donor functionality is essential for inhibitory activity. For example, compounds **12**, **13**, and **15** bore a hydroxyl-substituted benzene ring B and are active. In contrast, their derivatives, compounds **17**, **22**, and **45** either lacked this functionality or it was shielded by a methyl group to form an ether (compound **17**). The same tendency was present among the phenylbenzenesulfonamides and -sulfonates in comparison with inactive compounds from the same scaffold (Table 2). In addition, substituents longer than two atoms in the benzene ring decreased the compounds inhibitory activity or rendered the compound inactive (compounds **36−39**). Therefore, we observed that, ideally, 17β-HSD2 inhibitors contain an HBD feature directly linked to an aromatic ring B. The highest activity was gained when this functionality is in meta-position of the benzene ring, followed by ortho- and para-positions. The importance of this HBD feature was also confirmed with the SAR-pharmacophore model. Visual inspections of the substitution pattern of the A benzene ring suggested that hydrophobic substituents (*tert*-butyl, multiple methyl substituents) were well tolerated, whereas hydrogen-bond-forming functionalities decreased the activity.

To determine if our newly discovered 17β-HSD2 inhibitors could be unspecific, multitarget inhibitors interfering with many proteins, we applied a pan assay interference compounds (PAINS) filter.[47] This PAINS filter contains substructures that can possibly interfere with the biological assay by absorbing specific UV wavelengths, sticking to the unspecific binding sites, or interfering with singlet oxygen that is often transferred in certain high-throughput-screening assays. Two of our original hits, compounds **11** and **13**, were recognized as potential PAINS.[47] Compound **11** hitted filters 282:hzone_phenol_A(479) and 283:hzone_phenol_B(215), whereas compound **13** matched with filter 392:sulfonamideB(41). Both of these substructures are chromophores and therefore most likely predicted as PAINS. However, chromophoric compounds do not interfere with the biological assays used in this study. The enzyme activity was measured in the presence of the radiolabeled ligand, and the amounts of the substrate and product were detected by scillantation counting, measuring the ³H activity. Therefore, the presence of a possible chromophore does not interfere with the assay, unlike in the HTS methods described by Baell and Holloway.[47] Moreover, compounds having the same substructures as **11** and **13** were also evaluated against 17β-HSD2 activity, and they were weakly active or inactive (such as **29** and **30**, and **47** and **48**). This also indicates that compounds **11** and **13** are true positive hits.

CONCLUSION

In the present project, specific pharmacophore models for 17β-HSD2 inhibitors were developed. Using these models as virtual screening filters, 7 novel 17β-HSD2 inhibitors were discovered. An additional search for structurally similar compounds resulted in the biological evaluation of 28 small molecules. In total, 13 new 17β-HSD2 inhibitors, from which 10 represented phenylbenzenesulfonamides and -sulfonates, were discovered. To the best of our knowledge, this scaffold has not been reported previously in the literature as 17β-HSD2 inhibitors. These inhibitors aided in the development of the SAR model and rules for this specific scaffold: in general, 17β-HSD2 inhibitors need to have an HBD functionality on the meta-position of one benzene ring, and hydrophobic substituents on the other.

This study proved that pharmacophore modeling is a powerful tool in predicting activities and setting priorities for virtual screening. However, quality evaluation of the pharmacophore models revealed that model 1 outperformed the other two models in finding actives. Therefore, model 1 will be further refined for better sensitivity and specificity and used for further virtual screening campaigns.

■ MATERIALS AND METHODS

Data Sets. For the ligand-based pharmacophore modeling, a test set from the literature was collected. The aim was to collect structurally diverse, active compounds, which were shown to inhibit 17β-HSD2 in lysed cells. In contrast, all the inactive compounds had to be tested against 17β-HSD2 activity and be structurally similar to the actives. The final test set including the training molecules consisted of 15 17β-HSD2 inhibitors and 30 compounds that were inactive toward 17β-HSD2[22−25,31,48−52] (see Supporting Information Table S1 for structures and activities). The 2D structures of these compounds were drawn with ChemBioDraw Ultra 12.0.[53] For each molecule, a maximum of 500 conformations was generated with OMEGA-best settings (www.eyesopen.com,[54−56]) incorporated in LigandScout 3.03b (www.inteligand.com[57]).

For virtual screening campaigns, the SPECS database was downloaded from the SPECS Web site (www.specs.net). This commercial database is composed of small synthetic chemicals and consists of 202 906 compounds for which the company had at least 10 mg quantities in stock in January 2012. These compounds were transformed into a LigandScout database using the idbgen-tool of LigandScout. The database was generated using OMEGA-fast settings and calculating a maximum of 25 conformers/molecule (www.eyesopen.com,[54−56]). For the search for phenylbenzenesulfonamides and -sulfonates fitting model 1, the SPECS database version May 2013 (*n* = 197 475) was downloaded from the SPECS Web site and transformed into a multiconformational 3D database as described for the January 2012 version.

Pharmacophore Modeling. The pharmacophore models were constructed using LigandScout 3.0b (www.inteligand.com[57]). For the training set compounds, 500 conformations were created with OMEGA-best settings,[54−56] implemented in LigandScout. The program was set to create ten shared feature pharmacophore hypotheses from each of the training sets. In a shared feature pharmacophore model generation, LigandScout generates pharmacophore models from the chemical functionalities of the training compounds and aligns the molecules according to their pharmacophores.[58] Only features present in all training molecules are considered for model building. For the best alignment, common pharmacophore features are generated and assembled together, comprising the final pharmacophore model. The shared feature pharmacophore models contain only chemical features present in all the training molecules. The number of common chemical features naturally decreases when there are more training molecules, especially when using diverse ones. During this study, we started with larger training sets. However, when the training set contained more than two compounds, the obtained pharmacophore model became too general with only few features and low restrictivity, finding all the inactive compounds from the data set. The best of the generated hypotheses were selected for further refinement (removing features, setting features optional, adding XVOLs; for a general model refinement workflow, see ref 32), aiming to train each model to find only the active compounds and exclude the inactive ones from fitting. The quality of the

pharmacophore models was quantitatively evaluated by calculating the selectivity (eq 1) and specificity (eq 2) for each model separately and for a combination of multiple models.

$$\text{sensitivity} = \frac{\text{found actives}}{\text{all actives in the database}} \quad (1)$$

$$\text{specificity} = \frac{\text{found inactives}}{\text{all inactives in the database}} \quad (2)$$

Virtual Screening and Selection of the Hits. Virtual screening of the SPECS database (www.specs.net) was performed using LigandScout 3.0b. The original hit lists were filtered using Pipeline Pilot[59] to reduce the number of hits. The modified Lipinski-filter was set to pass all the compounds with molecular weight 250−500 g/mol, AlogP 1−6, more than two rotatable bonds, more than two HBAs, and less than three HBDs. Then the hit lists were clustered using DiscoveryStudio 3.0 (www.accelrys.com[60]). The program was set to create ten clusters for each hit list using function class fingerprints of maximum diameter 6 (FCFP_6) fingerprints.

Similarity Search. The search for the similar compounds for each of the active hits found in the first screening run was performed within SciFinder,[61] using the Explore Substances−Similarity search tool. For each of the new inhibitors, the compounds with similarity score ≥70 were collected. From these compounds, the ones that were commercially available from SPECS and had a modified substitution pattern (such as methyl group into ether or hydroxyl to methyl ether) were purchased and biologically evaluated. For the search for phenylbenzenesulfonamides and -sulfonates fitting model 1, the SPECS database version May 2013 was virtually screened using LigandScout 3.0b with model 1 only.

Screening against PAINS. To evaluate virtual screening libraries against PAINS,[47] our original 29 compounds were screened against the PAINS filter using the program KNIME.[62] The PAINS filters in SMILES format were downloaded from http://blog.rguha.net/?p=850, and the KNIME script for PAINS filtering[63] from http://www.myexperiment.org/workflows/1841.html.

Pharmacophore Model and Compound Alignments in 17β-HSD1. The new 17β-HSD2 inhibitors, model 1, and the SAR were evaluated against the 17β-HSD1 structure (PDB code 3HB5.[46] All the alignments were performed using LigandScout3.0b. The ligand from the protein was copied to the "alignment view", set as references, and aligned by features with model 1 or the SAR model. Then one of the models was set as reference structure, and all the active compounds were aligned to the model. After this, all the models and the compounds were copied into the ligand-binding pocket in the "structure-based view". On the basis of these alignments, the models and the compounds were visually analyzed against the 17β-HSD1 structure.

Literature Survey for Active Compounds. To search whether or not our active hit molecules have been reported in the literature previously, a SciFinder search was performed. Each of the active compounds was drawn in the SciFinder Structure editor, and an exact structure search was performed. In case a compound already had references, these were downloaded and further investigated.

Preparation of Inhibitors and Cytotoxicity Assessment. Inhibitors were dissolved in DMSO to obtain 20 mM stock solutions. For solubility reasons, compound AH-487/15020191 (see Supporting Information Table S1 for structure) was dissolved in chloroform. Further dilutions to the end concentration of 200 μM were prepared in TS2 buffer (100 mM NaCl, 1 mM EGTA, 1 mM EDTA, 1 mM MgCl₂, 250 mM sucrose, 20 mM Tris-HCl, pH 7.4).

To exclude that decreased enzyme activity might be due to unspecific toxicity, all compounds were tested at a concentration of 20 μM in intact HEK-293 cells for their effect on cell number, nuclear size, membrane permeability, and lysosomal mass. Cells grown in 96-well plates were incubated with compounds for 24 h, followed by addition of 50 μL of staining solution (Dulbecco's modified Eagle medium (DMEM) containing 2.5 μM Sytox-Green, 250 nM LysoTracker-Red, and 500 nM Hoechst-33342), rinsing twice with PBS and fixation with 4% paraformaldehyde. Plates were analyzed using a Cellomics ArrayScan high-content screening system using Bioapplication software according

to the manufacturer (Cellomics ThermoScientific, Pittsburgh, PA). None of the compounds altered these parameters.

Preparation of Cell Lysates. HEK-293 cells were transfected by the calcium phosphate precipitation method with plasmids for human 17β-HSD1, 17β-HSD2, or 11β-HSD2. Cells were cultivated for 48 h, washed with phosphate-buffered saline, and centrifuged for 4 min at 150g. After removal of the supernatants, cell pellets were snap frozen in dry ice and stored at −80 °C until further use.

17β-HSD1 and 17β-HSD2 Activity Measurements Using Cell Lysates. Lysates of human embryonic kidney cells (HEK-293) expressing either 17β-HSD1 or 17β-HSD2 were incubated for 10 min at 37 °C in TS2 buffer in a final volume of 22 μL containing either solvent (0.2% DMSO/chloroform) or the inhibitor at the respective concentration. N-(3-Methoxyphenyl)-N-methyl-5-m-tolylthiophene-2-carboxamide (compound **19** in ref 26) and apigenin[50] were used as positive controls for 17β-HSD1 and 17β-HSD2, respectively, in all experiments. 17β-HSD1 activity was measured in the presence of 190 nM unlabeled estrone, 10 nM radiolabeled estrone, and 500 μM NADPH. In contrast, 17β-HSD2 activity was determined in the presence of 190 nM unlabeled estradiol, 10 nM radiolabeled estradiol, and 500 μM NAD⁺. Reactions were stopped after 10 min by adding an excess of unlabeled estradiol and estrone (1:1, 2 mM in methanol). Possible promiscuous enzyme inhibition by aggregate formation of the chemicals was excluded by measuring the inhibition of the enzyme activity by the compounds in the presence of 0.1% Triton X-100.[36] The presence of the detergent did not affect the inhibitory effect of any of the compounds investigated. To exclude irreversible inhibition by the compounds investigated,[35] cell lysates were preincubated with the compounds for 0, 10, and 30 min, respectively, followed by measurement of the enzyme activity. Preincubation did not affect the inhibitory effects of any of the compounds investigated. The steroids were separated by TLC, followed by scintillation counting and calculation of substrate concentration. Data were collected from at least three independent measurements.

11β-HSD1 and 11β-HSD2 Activity Measurements Using Cell Lysates. The methods to determine 11β-HSD1 and -2 activity were performed as described previously.[64] Briefly, lysates of stably transfected cells, expressing either 11β-HSD1 or 11β-HSD2, were incubated for 10 min at 37 °C in TS2 buffer in a final volume of 22 μL containing either solvent (0.2% DMSO) or the inhibitor at the respective concentration. The nonselective 11β-HSD inhibitor glycyrrhetinic acid was used as positive control. Activity measurements of 11β-HSD1 were performed with 190 nM unlabeled cortisone, 10 nM radiolabeled cortisone, and 500 μM NADPH. To measure 11β-HSD2 activity, lysates were incubated with 40 nM unlabeled cortisol, 10 nM radiolabeled cortisol, and 500 μM NAD⁺. Reactions were stopped after 10 min by adding an excess of unlabeled cortisone and cortisol (1:1, 2 mM in methanol). The steroids were separated by TLC, followed by scintillation counting and calculation of substrate concentration. Data were collected from at least three independent measurements.

17β-HSD2 and 17β-HSD3 Activity Measurement in Intact Cells. Human embryonic kidney cells (HEK-293) were cultivated in DMEM containing 4.5 g/L glucose, 10% fetal bovine serum, 100 U/mL penicillin, 0.1 mg/mL streptomycin, 1× MEM nonessential amino acids, and 10 mM HEPES buffer, pH 7.4. The cells were incubated at 37 °C until 80% confluency. The cells were transfected using the calcium phosphate method with expression plasmids for 17β-HSD2 and 17β-HSD3. After 24 h, the cells were trypsinized and seeded on poly-L-lysine-coated 96-well plates (15 000 cells/well).

The inhibitory activities were measured 24 h after seeding as follows: old medium was aspirated and replaced by 30 μL of charcoal-treated DMEM (cDMEM). Ten microliters of inhibitor dissolved in cDMEM into the respective concentration was added, and mixtures were preincubated at 37 °C for 20 min. 17β-HSD2 inhibitory activities were measured in the presence of 190 nM unlabeled estradiol and 10 nM radiolabeled estradiol. N-(3-Methoxyphenyl)-N-methyl-5-m-tolylthio-phene-2-carboxamide (compound **19** in ref 26) was used as positive control. The reaction mixtures were incubated for 20 min, and the reactions were stopped by adding an excess of estradiol and estrone (1:1, 2 mM in methanol) to the mixture.

17β-HSD3 inhibitory activities were measured in the presence of 190 nM unlabeled androstenedione and 10 nM radiolabeled androstenedione. Benzophenone-1 was used as positive control[65]. The reaction mixtures were incubated for 30 min, and the reactions were stopped by adding an excess of androstenedione and testosterone (1:1, 2 mM in methanol). The steroids were separated by TLC, followed by scintillation counting and calculation of substrate concentration. Data was obtained from three independent measurements.

Characterization of Compounds 9−16 and 20−24. The infrared spectra of the 13 active compounds were recorded with a Bruker ALPHA equipped with a PLATINUM-ATR unit (spectral range 4000−400 cm^{-1}, 4 scans per cm^{-1}, Opus 7 software). The melting behavior of the substances was observed with an Olympus BH2 polarization microscope (Olympus Optical, J) equipped with a Kofler hot stage (Reichert, Vienna, Austria). The temperature calibration of the hot stage was performed with a series of melting point standards such as azobenzene (T_{fus}: 68 °C), acetanilide (T_{fus}: 114.5 °C), benzanilide (T_{fus}: 163 °C), and saccharin (T_{fus}: 228 °C). The compound characterization data are available in the Supporting Information.

ASSOCIATED CONTENT

Ⓢ Supporting Information

Compounds included in the test set and all the compounds tested for 17β-HSD2 activity during this study. For the active compounds additional data such as purity, melting points, calculated log$P$ values, NMR, and LC-MS data as provided by the supplier as well as their infrared spectra are given. This material is available free of charge via the Internet at http://pubs.acs.org.

AUTHOR INFORMATION

Corresponding Authors

*(Computational) Phone: +43-512-507-58253. Fax: +43-512-507-58299. E-mail: Daniela.Schuster@uibk.ac.at.
*(Biology) Phone: + 41 61 267 15 30. Fax: + 41 61 267 15 15. E-mail: Alex.Odermatt@unibas.ch.

Notes

The authors declare no competing financial interest.

ACKNOWLEDGMENTS

ABBREVIATIONS USED

AR, aromatic ring; H, hydrophobic feature; HSD, hydroxysteroid dehydrogenase; HBA, hydrogen bond acceptor; HBD, hydrogen bond donor; NI, negatively ionizable; PI, positively ionizable; SAR, structure−activity relationship; SDR, short chain reductase/dehydrogenase; XVOL, exclusion volume

REFERENCES

(1) Reginster, J.-Y.; Burlet, N. Osteoporosis: A still increasing prevalence. *Bone* **2006**, *38*, S4−S9.

(2) Glaser, D.; Kaplan, F. Osteoporosis. Definition and clinical presentation. *Spine (Philadelphia)* **1997**, *22* (24 suppl), 12S−16S.

(3) Compston, J. E. Sex Steroids and Bone. *Phys. Rev.* **2001**, *81*, 419−447.

(4) Riggs, B.; Khosia, S.; Melton, L. r. A unitary model for involutional osteoporosis: Estrogen deficiency causes both type I and type II osteoporosis in postmenopausal women and contributes to bone loss in aging men. *J. Bone Miner. Res.* **1998**, *13*, 763−773.

(5) Chin, K.-Y.; Ima-Nirwana, S. Sex steroids and bone health status in men. *Int. J. Endocrinol.* **2012**, *2012*, 208719.

(6) Michael, H.; Härkönen, P. L.; Väänänen, H. K.; Hentunen, T. A. Estrogen and testosterone use different cellular pathways to inhibit osteoclastogenesis and bone resorption. *J. Bone Miner. Res.* **2005**, *20*, 2224−2232.

(7) Kanis, J. A.; McCloskey, E. V.; Johansson, H.; Cooper, C.; Rizzoli, R.; Reginster, J.-Y. European guidance for the diagnosis and management of osteoporosis in postmenopausal women. *Osteoporosis Int.* **2012**, *24*, 23−57.

(8) Lewiecki, E. Current and emerging pharmacologic therapies for the management of postmenopausal osteoporosis. *J. Womens Health* **2009**, *18*, 1615−1626.

(9) Marjoribanks, J.; Farguhar, C.; Roberts, H.; Lethaby, A. Long term hormone therapy for perimenopausal and postmenopausal women. *Cochrane Database Syst. Rev.* **2012**, *11*, CD004143.

(10) Janssen, J. M. M. F.; Bland, R.; Hewison, M.; Coughtrie, M. W. H.; Sharp, S.; Arts, J.; Pols, H. A. P.; van Leeuwen, J. P. T. M. Estradiol Formation by Human Osteoblasts via Multiple Pathways: Relation with Osteoblast Function. *J. Cell. Biochem* **1999**, *75*, 528−537.

(11) Dong, Y.; Qiu, Q. Q.; Debear, J.; Lathrop, W. F.; Bertolini, D. R.; Tamburini, P. P. 17β-Hydroxysteroid dehydrogenases in human bone cells. *J. Bone Miner. Res.* **1998**, *13*, 1539−1546.

(12) Takeyama, J.; Sasano, H.; Suzuki, T.; Iinuma, K.; Nagura, H.; Andersson, S. 17β-Hydroxysteroid dehydrogenase types 1 and 2 in human placenta: An immunohistochemical study with correlation to placental development. *J. Clin. Endocrinol. Metab.* **1998**, *83*, 3710−3715.

(13) Mustonen, M. V.; Isomaa, V. V.; Vaskivuo, T.; Tapanainen, J.; Poutanen, M. H.; Stenbäck, F.; Vihko, R. K.; Vihko, P. T. Human 17beta-hydroxysteroid dehydrogenase type 2 messenger ribonucleic acid expression and localization in term placenta and in endometrium during the menstrual cycle. *J. Clin. Endocrinol. Metab.* **1998**, *83*, 1319−1324.

(14) Elo, J. P.; Akinola, L. A.; Poutanen, M.; Vihko, P.; Kyllönen, A. P.; Lukkarinen, O.; Vihko, R. Characterization of 17beta-hydroxysteroid dehydrogenase isoenzyme expression in benign and malignant human prostate. *Int. J. Cancer* **1996**, *66*, 37−41.

(15) Mustonen, M. V. J.; Poutanen, M. H.; Kellokumpu, S.; de Launoit, Y.; Isomaa, V. V.; Vihko, R. K.; Vihko, P. T. Mouse 17β-hydroxysteroid dehydrogenase type 2 mRNA is predominantly expressed in hepatocytes and in surface epithelial cells of the gastrointestinal and urinary tracts. *J. Mol. Endocrinol.* **1998**, *20*, 67−74.

(16) Bagi, C. M.; Wood, J.; Wilkie, D.; Dixon, B. Effect of 17β-hydroxysteroid dehydrogenase type 2 inhibitor on bone streght in ovariectomized cynomolgus monkeys. *J. Musculoskeletal Neuronal Interact.* **2008**, *8*, 267−280.

(17) Wu, L.; Einstein, M.; Geissler, W. M.; Chan, H. K.; Elliston, K. O.; Andersson, S. Expression cloning and characterization of human 17β-hydroxysteroid dehydrogenase type 2, a microsomal enzyme posessing 20α-hydroxysteroid dehydrogenase activity. *J. Biol. Chem.* **1993**, *268*, 12964−12639.

(18) Puranen, T. J.; Kurkela, R. M.; Lakkakorpi, J. T.; Poutanen, M. H.; Itäranta, P. V.; Melis, J. P. J.; Ghosh, D.; Vihko, R. K.; Vihko, P. T. Characterization of molecular and catalytic properties of intact and truncated human 17β-hydroxysteroid dehydrogenase type 2 enzymes: Intracellular localization of the wild-type enzyme in the endoplasmic reticulum. *Endocrinology* **1999**, *140*, 3334−3341.

(19) Labrie, F.; Luu-The, V.; Lin, S.-X.; Labrie, C.; Simard, J.; Breton, R.; Bélanger, A. The key role of 17β-hydroxysteroid dehydrogenases in sex steroid biology. *Steroids* **1997**, *62*, 148−158.

(20) Wu, X.; Lukacik, P.; Kavanagh, K. L.; Oppermann, U. SDR-type human hydroxysteroid dehydrogenases involved in steroid hormone action. *Mol. Cell. Endocrinol.* **2007**, *265−266*, 71−76.

(21) Kavanagh, K. L.; Jörnvall, H.; Persson, B.; Oppermann, U. The SDR superfamily: Functional and structural diversity within a family of metabolic and regulatory enzymes. *Cell. Mol. Life Sci.* **2008**, *65*, 3895−3906.

(22) Xu, K.; Al-Soud, Y. A.; Wetzel, M.; Hartmann, R. W.; Marchais-Oberwinkler, S. Triazole ring-opening leads to the discovery of potent nonsteroidal 17β-hydroxysteroid dehydrogenase type 2 inhibitors. *Eur. J. Med. Chem.* **2011**, *46*, 5978−5990.

(23) Wetzel, M.; Marchais-Oberwinkler, S.; Hartmann, R. W. 17β-HSD2 inhibitors for the treatment of osteoporosis: Identification of a promising scaffold. *Bioorg. Med. Chem.* **2011**, *19*, 807−815.

(24) Wood, J.; Bagi, C. M.; Akuche, C.; Bacchiocchi, A.; Baryza, J.; Blue, M.-L.; Brennan, C.; Campbell, A.-M.; Choi, S.; Cook, J. H.; Conrad, P.; Dixon, B. R.; Ehrlich, P. P.; Gane, T.; Gunn, D.; Joe, T.; Johnson, J. S.; Jordan, J.; Kramss, R.; Liu, P.; Levy, J.; Lowe, D. B.; McAlexander, I.; Natero, R.; Redman, A. M.; Scott, W. J.; Town, C.; Wang, M.; Wang, Y.; Zhang, Z. 4,5-Disubstituted *cis*-pyrrolidinones as inhibitors of type II 17β-hydroxysteroid dehydrogenase. Part 3. Identification of lead candidate. *Bioorg. Med. Chem. Lett.* **2006**, *16*, 4965−4968.

(25) Oster, A.; Klein, T.; Werth, R.; Kruchten, P.; Bey, E.; Negri, M.; Marchais-Oberwinkler, S.; Frotscher, M.; Hartmann, R. W. Novel estrone mimetics with high 17β-HSD1 inhibitory activity. *Bioorg. Med. Chem.* **2010**, *18*, 3494−3505.

(26) Marchais-Oberwinkler, S.; Xu, K.; Wetzel, M.; Perspicace, E.; Negri, M.; Meyer, A.; Odermatt, A.; Möller, G.; Adamski, J.; Hartmann, R. W. Structural optimization of 2,5-thiophene amides as highly potent and selective 17β-hydroxysteroid dehydrogenase type 2 inhibitors for the treatment of osteoporosis. *J. Med. Chem.* **2012**, *56*, 167−181.

(27) Al-Soud, Y. A.; Marchais-Oberwinkler, S.; Frotscher, M.; Hartmann, R. W. Synthesis and biological evaluation of phenyl substituted 1H-1,2,4-triazoles as non-steroidal inhibitors of 17β-hydroxysteroid dehydrogenase type 2. *Arch. Pharm.* **2012**, *345*, 610−621.

(28) Wermuth, C. G.; Ganellin, C. R.; Lindberg, P.; Mitscher, L. A. Glossary of terms used in medicinal chemistry (IUPAC Recommendations). *Pure Appl. Chem.* **1998**, *70*, 1129−1143.

(29) Gao, Q.; Yang, L.; Zhu, Y. Pharmacophore based drug design approach as a practical process in drug discovery. *Curr. Comput.-Aided Drug Des.* **2010**, *6*, 37−49.

(30) Schuster, D.; Waltenberger, B.; Kirchmair, J.; Distinto, S.; Markt, P.; Stuppner, H.; Rollinger, J. M.; Wolber, G. Predicting cyclooxygenase inhibition by three-dimentional pharmacophoric profiling. Part I: Model generation, validation and applicability in ethnopharmacology. *Mol. Inf.* **2010**, *1*, 79−90.

(31) Bydal, P.; Auger, S.; Poirier, D. Inhibition of type 2 17beta-hydroxysteroid dehydrogenase by estradiol derivatives bearing a lactone on the D-ring: Structure-activity relationships. *Steroids* **2004**, *69*, 325−342.

(32) Vuorinen, A.; Nashev, L. G.; Odermatt, A.; Rollinger, J. M.; Schuster, D. Pharmacophore model refinement for 11β-hydroxysteroid dehydrogenase inhibitors: Search for modulators of intracellular glucocorticoid concentrations. *Mol. Inf.* **2014**, *33*, 15−25.

(33) Lipinski, C. A.; Lombardo, F.; Dominy, B. W.; Feeney, P. J. Experimental and computational approaches to estimate solubility and permeabilityy in drug discovery and development settings. *Adv. Drug Delivery Rev.* **2001**, *46*, 3−26.

(34) Organic Chemistry Portal. *OSIRIS Property Explorer*; Actelion Pharmaceuticals Ltd., Gewerbestrasse 16, 4123 Allschwil, Switzerland.

(35) Atanasov, A. G.; Tam, S.; Rocken, J. M.; Baker, M. E.; Odermatt, A. Inhibition of 11 beta-hydroxysteroid dehydrogenase type 2 by dithiocarbamates. *Biochem. Biophys. Res. Commun.* **2003**, *308*, 257−62.

(36) McGovern, S. L.; Helfand, B. T.; Feng, B.; Shoichet, B. K. A Specific Mechanism of Nonspecific Inhibition. *J. Med. Chem.* **2003**, *46*, 4265−4272.

(37) Odermatt, A.; Kratschmar, D. V. Tissue-specific modulation of mineralocorticoid receptor function by 11β-hydroxysteroid dehydrogenases: An overview. *Mol. Cell. Endocrinol.* **2012**, *350*, 168−86.

(38) Geissler, W. M.; Davis, D. L.; Wu, L.; Bradshaw, K. D.; Patel, S.; Mendonca, B. B.; Elliston, K. O.; Wilson, J. D.; Russell, D. W.; Andersson, S. Male pseudohermaphroditism caused by mutations of testicular 17beta-hydroxysteroid dehydrogenase 3. *Nat. Genet.* **1994**, *7*, 34−39.

(39) Halperin, J. A.; Natarajan, A.; Aktas, H.; Fan, Y.-H. C., Preparation of 3-3-di-substituted oxindoles as inhibitors of translation initiation. Patent WO 2005080335 A1, January 9, 2005.

(40) Xu, F.; Xu, H.; Wang, X.; Zhang, L.; Wen, Q.; Zhang, Y.; Xu, W. Discovery of N-(3-((7H-purin-6-yl)thio)-4-hydroxynaphthalen-1-yl)-sulfonamide derivatives as novel protein kinase and angiogenesis inhibitors for the treatment of cancer: Synthesis and biological evaluation. Part III. *Bioorg. Med. Chem.* **2014**, *22*, 1487−1495.

(41) Kotelevtsev, Y.; Brown, R. W.; Fleming, S.; Kenyon, C.; Edwards, C. R. W.; Seckl, J. R.; Mullins, J. J. Hypertension in mice lacking 11β-hydroxysteroid dehydrogenase type 2. *J. Clin. Invest.* **1999**, *103*, 683−689.

(42) Wang, M. Inhibitors of 11β-Hydroxysteroid Dehydrogenase Type 1 in Antidiabetic Therapy. In *Diabetes - Perspectives in Drug Therapy*; Schwanstecher, M., Ed.; Springer: Berlin, 2011; Vol. 203, pp 127−146.

(43) Andersson, S.; Geissler, W. M.; Patel, S.; Wu, L. The molecular biology of androgenic 17β-hydroxysteroid dehydrogenases. *J. Steroid Biochem. Mol. Biol.* **1995**, *53*, 37−39.

(44) Koh, E.; Noda, T.; Kanaya, J.; Namiki, M. Differential expression of 17β-hydroxysteroid dehydrogenase isozyme genes in prostate cancer and noncancer tissues. *Prostate* **2002**, *53*, 154−159.

(45) Berman, H. M.; Westbrook, J.; Feng, Z.; Gilliland, G.; Bhat, T. N.; Weissig, H.; Shindayalov, I. N.; Bourne, P. E. The Protein Data Bank. *Nucl. Acids. Res.* **2000**, *28*, 235−242.

(46) Mazumdar, M.; Fournier, D.; Zhu, D. W.; Cadot, C.; Poirier, D.; Lin, S. X. Binary and ternary crystal structure analyses of a novel inhibitor with 17β-HSD type 1: a lead compound for breast cancer therapy. *Biochem. J.* **2009**, *424*, 357−366.

(47) Baell, J. B.; Holloway, G. A. New Substructure Filters for Removal of Pan Assay Interference Compounds (PAINS) from Screening Libraries and for Their Exclusion in Bioassays. *J. Med. Chem.* **2010**, *53*, 2719−2740.

(48) Lilienkampf, A.; Karkola, S.; Alho-Richmond, S.; Koskimies, P.; Johansson, N.; Huhtinen, K.; Vihko, K.; Wähälä, K. Synthesis and biological evaluation of 17β-hydroxysteroid dehydrogenase type 1 (17β-HSD1) inhibitors based on a thieno[2,3-d]pyrimidin-4(3H)-one core. *J. Med. Chem.* **2009**, *52*, 6660−6671.

(49) Allan, G. M.; Lawrence, H. R.; Cornet, J.; Bubert, C.; Fischer, D. S.; Vicker, N.; Smith, A.; Tutill, H. J.; Purohit, A.; Day, J. M.; Mahon, M. F.; Reed, M. J.; Potter, B. V. L Modification of estrone at the 6, 16, and 17 positions: Novel potent inhibitors of 17β-hydroxysteroid dehydrogenase type 1. *J. Med. Chem.* **2006**, *49*, 1325−1345.

(50) Schuster, D.; Nashev, L. G.; Kirchmair, J.; Laggner, C.; Wolber, G.; Langer, T.; Odermatt, A. Discovery of nonsteroidal 17β-hydroxysteroid dehydrogenase 1 inhibitors by pharmacophore-based screening of virtual compound libraries. *J. Med. Chem.* **2008**, *51*, 4188−4199.

(51) Schuster, D.; Kowalik, D.; Kirchmair, J.; Laggner, C.; Markt, P.; Aebischer-Gumy, C.; Ströhle, F.; Möller, G.; Wolber, G.; Wilckens, T.; Langer, T.; Odermatt, A.; Adamski, J. Identification of chemically diverse, novel inhibitors of 17β-hydroxysteroid dehydrogenase type 3 and 5 by pharmacophore-based virtual screening. *J. Steroid Biochem. Mol. Biol.* **2011**, *125*, 148−161.

(52) Fischer, D. S.; Allan, G. M.; Bubert, C.; Vicker, N.; Smith, A.; Tutill, H. J.; Purohit, A.; Wood, L.; Packham, G.; Mahon, M. F.; Reed, M. J.; Potter, B. V. L E-ring modified steroids as novel potent inhibitors of 17β-hydroxysteroid dehydrogenase type 1. *J. Med. Chem.* **2005**, *48*, 5749−5770.

(53) *ChemBioDraw Ultra, 12.0*; CambridgeSoft, 1986−2010.

(54) *OMEGA, 2.2.3*; OpenEye Scientific Software, Santa Fe, NM.

(55) Hawkins, P. C. D.; Skillman, A. G.; Warren, G. L.; Ellingson, B. A.; Stahl, M. T. Conformer generation with OMEGA: Algorithm and validation using high quality structures from the protein databank and Cambridge Structural Database. *J. Chem. Inf. Model* **2010**, *50*, 572−584.

(56) Hawkins, P. C. D.; Nicholls, A. Conformer generation with OMEGA: Learning from the data set and the analysis of failures. *J. Chem. Inf. Model* **2012**, *52*, 2919−2936.

(57) Wolber, G.; Langer, T. LigandScout: 3-D pharmacophores derived from protein-bound ligands and their use as virtual screening filters. *J. Chem. Inf. Model* **2005**, *45*, 160−169.

(58) Wolber, G.; Dornhofer, A. A.; Langer, T. Efficient overlay of small organic molecules using 3D pharmacophores. *J. Comput.-Aided Mol. Des.* **2006**, *20*, 773−788.

(59) *Pipeline Pilot*; Accelrys Software Inc., 2010.

(60) *DiscoveryStudio, 3.0*; Accelrys Software Inc., 2005−2010.

(61) *SciFinder*; American Chemical Society, 2013.

(62) Berthold, M.; Cebron, N.; Dill, F.; Gabriel, T.; Kötter, T.; Meinl, T.; Ohl, P.; Sieb, C.; Thiel, K.; Wiswedel, B. KNIME: The Konstanz Information Miner. In *Data Analysis, Machine Learning and Applications*; Preisach, C.; Burkhardt, H.; Schmidt-Thieme, L.; Decker, R., Eds.; Springer: Berlin, 2008; pp 319−326.

(63) Saubern, S.; Guha, R.; Baell, J. B. KNIME Workflow to Assess PAINS Filters in SMARTS Format. Comparison of RDKit and Indigo Cheminformatics Libraries. *Mol. Inf.* **2011**, *30*, 847−850.

(64) Kratschmar, D. V.; Vuorinen, A.; Da Cunha, T.; Wolber, G.; Classen-Houben, D.; Doblhoff, O.; Schuster, D.; Odermatt, A. Characterization of activity and binding mode of glycyrrhetinic acid derivatives inhibiting 11β-hydroxysteroid dehydrogenase type 2. *J. Steroid Biochem. Mol. Biol.* **2011**, *125*, 129−142.

(65) Nashev, L. G.; Schuster, D.; Laggner, C.; Sodha, S.; Langer, T.; Wolber, G.; Odermatt, A. The UV-filter benzophenone-1 inhibits 17β-hydroxysteroid dehydrogenase type 3: Virtual screening as a strategy to identify potential endocrine disrupting chemicals. *Biochem. Pharmacol.* **2010**, *79*, 1189−1199.